Article

Au Nanocrystal Growth on Nanotubes Controlled by Conformations and Charges of Sequenced Peptide Templates

Ramin Djalali, Yung-fou Chen, and Hiroshi Matsui

J. Am. Chem. Soc., **2003**, 125 (19), 5873-5879• DOI: 10.1021/ja0299598 • Publication Date (Web): 17 April 2003

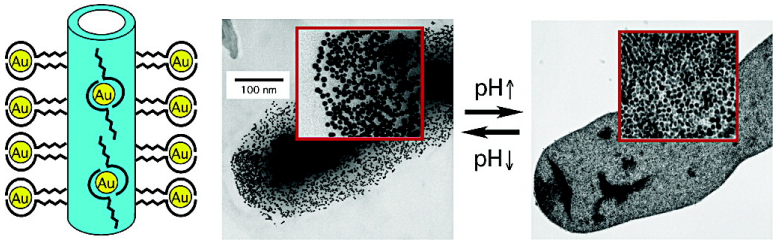

More About This Article

Additional resources and features associated with this article are available within the HTML version:

- Supporting Information
- Links to the 17 articles that cite this article, as of the time of this article download
- Access to high resolution figures
- Links to articles and content related to this article
- Copyright permission to reproduce figures and/or text from this article

View the Full Text HTML

J|A|C|S
ARTICLES
Published on Web 04/17/2003

Au Nanocrystal Growth on Nanotubes Controlled by Conformations and Charges of Sequenced Peptide Templates

Ramin Djalali, Yung-fou Chen, and Hiroshi Matsui*

Contribution from the Department of Chemistry and Biochemistry at Hunter College and the Graduate Center, The City University of New York, New York, New York 10021

Received December 30, 2002; E-mail: hmatsui@hunter.cuny.edu

Abstract: A new biological approach to fabricate Au nanowires was examined by using sequenced peptide nanotubes as templates. The sequenced histidine-rich peptide molecules were assembled on nanotubes, and the biological recognition of the sequenced peptide selectively trapped Au ions for the nucleation of Au nanocrystals. After Au ions were reduced, highly monodisperse Au nanocrystals were grown on nanotubes. The conformations and the charge distributions of the histidine-rich peptide, determined by pH and Au ion concentration in the growth solution, control the size and the packing density of Au nanocrystals. The diameter of Au nanocrystal was limited by the spacing between the neighboring histidine-rich peptides on nanotubes. A series of TEM images of Au nanocrystals on nanotubes in the shorter Au ion incubation time periods reveal that Au nanocrystals grow inside the nanotubes first and then cover the outer surfaces of nanotubes. Therefore, multiple materials will be coated inside and outside the nanotubes respectively by controlling doping ion concentrations and their deposition sequences. It should be noted that metallic nanocrystals in diameter around 6 nm are in the size domain to observe a significant conductivity change by changing the packing density, and therefore this system may be developed into a conductivity-tunable building block.

Introduction

There has been much interest lately in ordered two- and three-dimensional device fabrications by using nanowires as building blocks.[1−7] Those nanowires with various electronic transport properties can be synthesized in various phases with a variety of chemical methods, depending upon the materials used to form nanowires. While those nanowires have selectively been used as building blocks for specific device configurations, it would be practical if we can fabricate nanowires with various electrical properties in one simple method.

Nanocrystals are the materials that can tune their electronic structures via their size and morphology.[8−10] When the coupling strength of overlapped wave functions between neighboring nanocrystals is tuned by compressing the lattice of nanocrystals, the range of tuning the electronic structures is considerable because the overlap depends exponentially on the interdot distance and the size.[11,12] On the basis of this principle, various nanocrystals have been demonstrated to tune electrical, magnetic, and optical properties by controlling the size and the packing density of nanocrystals on planar surfaces.[13−27] The electronic structures of nanocrystals were also controlled by their shapes.[28−30] If nanocrystals can be formed into the nanowire geometry in controlled diameters and packing densities, one may be able to produce nanowires with tunable electrical properties

(1) Cui, Y.; Wei, Q. Q.; Park, H. K.; Lieber, C. M. *Science* **2001**, *293*, 1289.
(2) Huang, Y.; Duan, X.; Cui, Y.; Lauhon, L. J.; Kim, K. H.; Lieber, C. M. *Science* **2001**, *294*, 1313.
(3) Diehl, M. R.; Yaliraki, S. N.; Beckman, R. A.; Barahona, M.; Heath, J. R. *Angew. Chem., Int. Ed.* **2001**, *41*, 353.
(4) Collins, P. G.; Arnold, M. S.; Avouris, P. *Science* **2001**, *292*, 706.
(5) Bachtold, A.; Hadley, P.; Nakanishi, T.; Dekker, C. *Science* **2001**, *294*, 1317.
(6) Huynh, W. U.; Dittmer, J. J.; Alivisatos, A. P. *Science* **2002**, *295*, 2425.
(7) Ray, O.; Sirenko, A. A.; Berry, J. J.; Samarth, N.; Gupta, J. A.; Malajovich, I.; Awschalom, D. D. *Appl. Phys. Lett.* **2000**, *76*, 1167.
(8) Alivisatos, A. P. *Science* **1996**, *271*, 933.
(9) Alivisatos, A. P. *J. Phys. Chem.* **1996**, *100*, 13226.
(10) Landes, C. F.; Link, S.; Mohamed, M. B.; Nikoobakht, B.; El-Sayed, M. A. *Pure Appl. Chem.* **2002**, *74*, 1675.
(11) Remacle, F.; Levine, R. D. *J. Am. Chem. Soc.* **2000**, *122*, 4084.
(12) Remacle, F.; Beverly, K. C.; Heath, J. R.; Levine, R. D. *J. Phys. Chem. B* **2002**, *106*, 4116.
(13) Beverly, K. C.; Sample, J. L.; Sampaio, J. F.; Remacle, F.; Heath, J. R.; Levine, R. D. *Proc. Natl. Acad. Sci. U.S.A.* **2002**, *99*, 6456.
(14) Murray, C. B.; Kagan, C. R.; Bawendi, M. G. *Annu. Rev. Mater.* **2000**, *30*, 545.
(15) Murray, C. B.; Norris, D. J.; Bawendi, M. G. *J. Am. Chem. Soc.* **1993**, *115*, 8706.
(16) O'Brien, S.; Brus, L.; Murray, C. B. *J. Am. Chem. Soc.* **2001**, *123*, 12085.
(17) Puntes, V. F.; Krishnan, K. M.; Alivisatos, A. P. *Appl. Phys. Lett.* **2001**, *78*, 2187.
(18) Micic, O. I.; Jones, K. M.; Cahill, A.; Nozik, A. J. *J. Phys. Chem. B* **1998**, *102*, 9791.
(19) Harfenist, S. A.; Wang, Z. L.; Alvarez, M. M.; Vezmar, I.; Whetten, R. L. *J. Phys. Chem.* **1996**, *100*, 13904.
(20) Petit, C.; Taleb, A.; Pileni, M. P. *J. Phys. Chem. B* **1999**, *103*, 1805.
(21) Wong, K. K. W.; Douglas, T.; Gider, S.; Awschalom, D. D.; Mann, S. *Chem. Mater.* **1998**, *10*, 279.
(22) Liu, X. G.; Fu, L.; Hong, S. H.; Dravid, V. P.; Mirkin, C. A. *Adv. Mater.* **2002**, *14*, 231.
(23) Park, S.-J.; Taton, T. A.; Mirkin, C. A. *Science* **2002**, *295*, 1503.
(24) Yamamuro, S.; Farrell, D. F.; Majetich, S. A. *Phys. Rev. B* **2002**, *65*, 224431.
(25) Rengarajan, R.; Jiang, P.; Larrabee, D. C.; Colvin, V. L.; Mittleman, D. M. *Phys. Rev. B* **2001**, *64*, 205103.
(26) Doty, R. C.; Yu, H. B.; Shih, C. K.; Korgel, B. A. *J. Phys. Chem. B* **2001**, *105*, 8291.
(27) Tripp, S. L.; Pusztay, S. V.; Ribbe, A. E.; Wei, A. *J. Am. Chem. Soc.* **2002**, *124*, 7914.
(28) Peng, X. G.; Manna, L.; Yang, W. D.; Wickham, J.; Scher, E.; Kadavanich, A.; Alivisatos, A. P. *Nature* **2000**, *404*, 59.
(29) El-Sayed, M. A. *Acc. Chem. Res.* **2001**, *34*, 257.
(30) Murphy, C. J.; Jana, N. R. *Adv. Mater.* **2002**, *14*, 80.

from one type of nanocrystal. Because one synthetic method can be applied to form one type of nanocrystal and the size of nanocrystal can be controlled kinetically in the same synthetic method,[31,32] this proposed approach will allow us to produce nanowires with various electrical properties in one simple synthetic method. This outcome may also be important to engineer nanoscale electronic devices such as quantum computers from nanocrystals.[33]

One of the straightforward approaches to form nanocrystals into the nanowire geometry is to use template nanowires to grow nanocrystals on the nanowire surfaces. While nanocrystals can separately grow in solution and then mix with template nanowires to anchor nanocrystals onto nanowire surfaces via chemical interactions between capping ligands of nanocrystals and template nanowires,[34] it would be desirable to grow nanocrystals directly on nanowires in a simpler fabrication procedure. The difficulty for the one-step synthetic approach is to control the size and the density of nanocrystals on nanowire surfaces.

Biological systems control mineralizations and nanocrystal synthesis of various metals in the exact shapes and sizes with high reproducibility and accuracy.[35−40] Therefore, it is a logical approach to use biological nanotubes as templates to grow monodisperse nanocrystals on the nanowires via biomineralization.[41−47] Nanocrystal synthesis via biomineralization was so efficient that contamination with various precipitates was reduced significantly as compared to conventional electroless coating processes.[45] This feature is important because the contamination makes reproducible electronic transport and absorption measurements problematic.[48−50]

Histidine-containing peptides have been studied extensively because their high affinities to metal ions damage central nervous systems by altering peptide conformations into abnormal forms via histidine−metal complexation and this protein deformation may cause Parkinson's and Alzheimer's diseases.[51] It is advantageous to apply a nanotube-form of the sequenced histidine-rich peptides as a template for metallic nanowire synthesis because specific sequences of peptides mineralize specific metals/semiconductors to produce highly crystalline nanocrystals.[39] Another advantage is that peptide conformations and charges on nanotubes control the size and the packing density of nanocrystals.[45,52−55] In our previous publication, the sequenced histidine-rich peptides were formed into nanotubes by immobilizing them on template nanotubes.[45] The template nanotube, whose structure is shown in Figure 1a, is self-assembled from small bolaamphiphile peptide monomers (Figure 1b) in NaOH/citric acid solution via three-dimensional intermolecular hydrogen bonds among the monomers.[56−58] This template nanotube is programmed to immobilize biological molecules such as DNAs, peptides, and proteins at free amide sites of the sidewall via hydrogen bonding (Figure 1c).[59]

We have also demonstrated that an immobilized histidine-rich peptide, whose sequence is A−H−H−A−H−H−A−A−D, can mineralize Au nanocrystals on the nanotubes in the uniform size distribution.[45] The fabrication process is illustrated in Figure 2. Briefly, Au ions are captured by imidazole and amine groups of the sequenced peptides on the nanotubes (Figure 2b), and then the trapped Au ions in the peptides nucleate Au nanocrystals after reducing those ions by hydrazine hydrate (Figure 2c). Au nanocrystals grown on the nanotubes were highly monodisperse, and their average diameter was 6 nm. This system has potential to control the size and the packing density of nanocrystals on nanotubes by simply adjusting external experimental conditions such as pH, temperature, and ion concentration because immobilized peptides on nanotubes may have freedom to undergo the conformation change by changing the experimental conditions, which determines the nanocrystal size and the packing density.[54]

To examine this hypothesis, we studied the correlations between the growth conditions such as pH and ion concentrations and the size/packing density of Au nanocrystals grown on the sequenced histidine-rich peptide nanotubes. Both the ion concentration and the pH of the growth solution could be used to control the packing density of Au nanocrystals on the nanotubes, while the diameter of Au nanocrystals was always 6 nm, independent of the growth conditions. The mechanism to control the size and the packing density of nanocrystals on the nanotubes via the conformations and the charge distributions of the sequenced peptide is described in the Discussion section. It should be noted that metallic nanocrystals 6 nm in diameter are in the size domain to observe a significant conductivity change by changing the packing density, and therefore this system may be useful as a conductivity-tunable building block.[13]

Experimental Section

First, bis(*N*-α-amido-glycylglycine)-1,7-heptane dicarboxylate molecules (10 mM) were self-assembled into template nanotubes in a pH 5.5 citric acid/NaOH solution. Details of the heptane dicarboxylate synthesis and the heptane dicarboxylate nanotube self-assembly are

(31) Chen, C.-C.; Herhold, A. B.; Johnson, C. S.; Alivisatos, A. P. *Science* **1997**, *276*, 398.
(32) Mohamed, M. B.; Wang, Z. L.; El-Sayed, M. A. *J. Phys. Chem. A* **1999**, *103*, 10255.
(33) Wang, J. X.; Kais, S.; Remacle, F.; Levine, R. D. *J. Phys. Chem. B* **2002**, *106*, 12847.
(34) Matsui, H.; Pan, S.; Douberly, G. E. J. *J. Phys. Chem. B* **2001**, *105*, 1683.
(35) Baeuerlein, E. *Biomineralization*; Wiley-VCH: Cambridge, 2000.
(36) Mann, S. *Biomineralization*; Oxford University Press: New York, 2001.
(37) Niemeyer, C. M. *Angew. Chem., Int. Ed.* **2001**, *40*, 4128.
(38) Dujardin, E.; Mann, S. *Adv. Mater.* **2002**, *14*, 775.
(39) Slocik, J. M.; Moore, J. T.; Wright, D. W. *Nano Lett.* **2002**, *2*, 169.
(40) Gardea-Torresdey, J. L.; Parsons, J. G.; Gomez, E.; Peralta-Videa, J.; Troiani, H. E.; Santiago, P.; Yacaman, M. J. *Nano Lett.* **2002**, *2*, 397.
(41) Douglas, T.; Young, M. *Adv. Mater.* **1999**, *11*, 679.
(42) Shenton, W.; Douglas, T.; Young, M.; Stubbs, G.; Mann, S. *Adv. Mater.* **1999**, *11*, 253.
(43) Behrens, S.; Rahn, K.; Habicht, W.; Bohm, K.-J.; Rosner, H.; Dinjus, E.; Unger, E. *Adv. Mater.* **2002**, *14*, 1621.
(44) Lee, S. W.; Mao, C. B.; Flynn, C. E.; Belcher, A. M. *Science* **2002**, *296*, 892.
(45) Djalali, R.; Chen, Y.-f.; Matsui, H. *J. Am. Chem. Soc.* **2002**, *124*, 13660.
(46) Hartgerink, J. D.; Beniash, E.; Stupp, S. I. *Science* **2001**, *294*, 1684.
(47) Field, M.; Smith, C. J.; Awshalom, D. D.; Mayes, E. L.; Davis, S. A.; Mann, S. *Appl. Phys. Lett.* **1998**, *73*, 1739.
(48) Matsui, H.; Pan, S.; Gologan, B.; Jonas, S. *J. Phys. Chem. B* **2000**, *104*, 9576.
(49) Harnack, O.; Ford, W. E.; Yasuda, A.; Wessels, J. M. *Nano Lett.* **2002**, *2*, 919.
(50) Matsui, H.; Gologan, B.; Pan, S.; Douberly, G. J. *Eur. Phys. J. D* **2001**, *16*, 403.
(51) Pappalardo, G.; Impellizzeri, G.; Bonomo, R. P.; Campagna, T.; Grasso, G.; Saita, M. G. *New J. Chem.* **2002**, *26*, 593.
(52) Whaley, S. R.; English, D. S.; Hu, E. L.; Barbara, P. F.; Belcher, A. M. *Nature* **2000**, *405*, 665.
(53) Ziegler, J.; Chang, R. T.; Wright, D. W. *J. Am. Chem. Soc.* **1999**, *121*, 2395.
(54) Spreitzer, G.; Whitling, J. M.; Madura, J. D.; Wright, D. W. *Chem. Commun.* **2000**, 209.
(55) Whitling, J. M.; Spreitzer, G.; Wright, D. W. *Adv. Mater.* **2000**, *12*, 1377.
(56) Matsui, H.; Gologan, B. *J. Phys. Chem. B* **2000**, *104*, 3383.
(57) Shimizu, T.; Kogiso, M.; Masuda, M. *Nature* **1996**, *383*, 487.
(58) Shimizu, T.; Kogiso, M.; Masuda, M. *J. Am. Chem. Soc.* **1997**, *119*, 6209.
(59) Douberly, G. J.; Pan, S.; Walters, D.; Matsui, H. *J. Phys. Chem. B* **2001**, *105*, 7612.

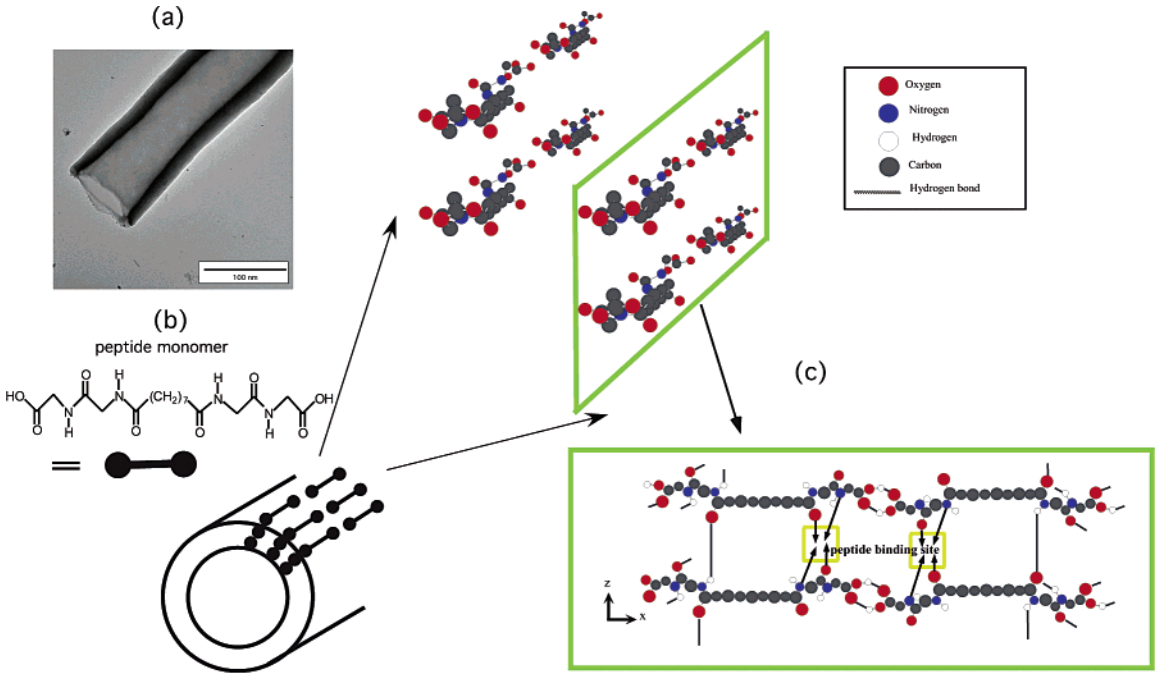

Figure 1. (a) TEM image of the template nanotube. (b) Chemical structure of peptide bolaamphiphile monomer. (c) Chemical structure of the template nanotube from the monomer (b). The template nanotube surface has free amide groups (shown by arrows and yellow squares) to immobilize biological molecules on the nanotube surfaces.

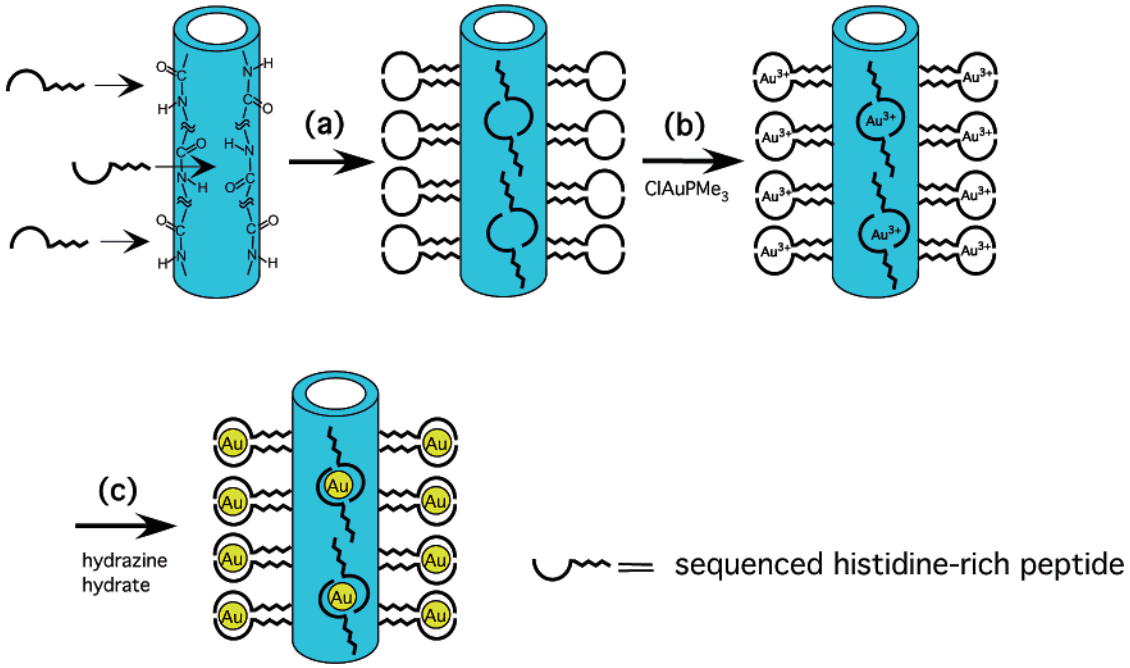

Figure 2. Scheme of the Au nanowire fabrication. (a) Immobilization of the sequenced histidine-rich peptide at the amide binding sites of the template nanotubes. (b) Au ion immobilization on the sequenced histidine-rich peptide. (c) Au nanocrystal growth on the nanotubes nucleated at Au ion-binding sites after reducing Au ions with hydrazine hydrate.

described elsewhere.[56] After the template nanotubes were washed with deionized water several times, a 1 mL solution of the template nanotube was mixed with a 1 mL solution of a sequenced histidine-rich peptide, A−H−H−A−H−H−A−A−D (2 μmol), in Tris buffer (0.1 M, pH 8.6) for 24 h to immobilize the histidine-rich peptide onto the nanotubes. This histidine-rich peptide was sequenced by Applied Biosystems Peptide Synthesizer 432A and purified with Beckman 110 HPLC with the C-18 reverse phase column at the CUNY Gene Center. After the histidine peptides were immobilized on the nanotube surfaces, citric acid (1 M) and NaOH (1 M) were added to the solution to adjust pH's in the range of 4−11.5. To grow Au nanocrystals on the histidine-rich peptide nanotubes, 5 mg of trimethylphosphinchlorogold salt ($ClAuPMe_3$) was mixed with the histidine-rich peptide nanotube solution (4 mL) in the dark at room temperature. The incubation time of Au ion was varied to control the Au ion concentration on the nanotubes between 5 h and 20 days. Next, 50 μmol of a reducing agent, hydrazine hydrate (2 M), was added to grow Au nanocrystals on the nanotubes. Transmission electron microscopy (TEM) was applied to resulting Au nanotubes in the dark field mode on a PHILLIPS CM-100 microscope operating at 80 keV. For the investigation, the nanotube solutions were dropped onto carbon coated copper grids and were allowed to dry gradually at room temperature.

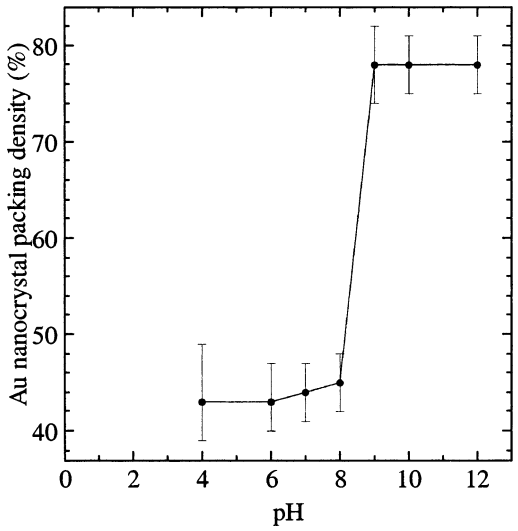

Figure 3. The correlation between the packing density of Au nanocrystals and pH of the growth solution.

Results

The Influence of pH upon Au Nanocrystal Growth on Nanotubes. To understand the influence of pH upon Au nanocrystal growth on the sequenced histidine-rich peptide nanotube, the precursor Au ion, $ClAuPMe_3$, was immobilized on the histidine-rich peptide nanotubes by incubating it in the nanotube solution for 10 days at various pH's before reducing with hydrazine hydrate. Hydrazine hydrate, one of the weaker reducing agents, was found to produce most monodisperse nanocrystals among various reducing agents. When Au ions were incubated in the nanotube solution between pH 4 and pH 8, the size of Au nanocrystals was 6 nm in diameter, and the packing density was 43% in area after reducing the Au ion−nanotube solutions (Figure 3).[60] Below pH 4, the sequenced peptide precipitated without coating the nanotubes, and therefore no Au nanocrystals were observed on the nanotubes. Figure 4a is a TEM image of Au nanocrystals on the nanotube by incubating the Au ion at pH 8. The inset of Figure 4a, the TEM image in higher magnification, shows that the shape of Au nanocrystals is isotropic and those nanocrystals are also highly monodisperse. A striking difference in the nanocrystal distribution was observed when the Au ions were incubated at pH's higher than 9. When Au ions were incubated in the pH range between 9 and 11.5, the packing density of Au nanocrystals was 78% in area (Figure 3), which is much higher than the packing density observed in the pH < 9 solutions, while the diameter of Au nanocrystals remained constant at 6 nm in the entire pH range examined in this study. Figure 4b shows a TEM image of Au nanocrystals on the nanotube by incubating the Au ion at pH 11.5. The magnified TEM image, the inset of Figure 4b, reveals the higher packing density of Au nanocrystals on the nanotube as compared to the packing density observed in the inset of Figure 4a.

The Influence of Au Ion Concentration upon Au Nanocrystal Growth on Nanotubes. Au nanocrystals were also grown on the sequenced histidine-rich peptide nanotubes in various precursor Au ion concentrations at pH 8, and the size and the packing density of Au nanocrystals were monitored after reducing those growth solutions. The relative concentration of the Au ion, $ClAuPMe_3$, on the nanotubes was controlled by the ion incubation time in the growth solution.[61] It means that the longer Au ion incubation corresponds to the higher relative concentration of Au ions on the nanotubes. When the nanotubes were incubated with the Au ions for 12 days, Au nanocrystals were grown to 6 nm in diameter, and the packing density was 54% in area (Figure 5a). The packing density of Au nanocrystals was reduced to 18% as the ion incubation time was shortened to 4 days (Figure 5b). While the packing density was considerably decreased with the 4 day-ion incubation, the size of Au nanocrystals still remained constant at 6 nm in diameter. The packing density further declined to 9% in area with no nanocrystal size change when the Au ion was incubated for 2 days (Figure 5c). The packing density of Au nanocrystals was observed to be proportional to the Au ion incubation time, as shown in Figure 6. There was no further change in the packing density of Au nanocrystals over 12 days.

While a series of TEM images were analyzed to understand the trend in Au nanocrystal growth on the nanotube in various Au ion concentrations, it was also interesting to observe darker cores within the central region of the nanotubes in those TEM images as shown in Figure 5a−c. The darker contrast may be observed due to the Au nanocrystal growth inside the template nanotubes. To confirm this hypothesis, the incubation time of Au ion was further reduced to 5 h. Under this condition, few Au nanocrystals were observed on the outer surface of the nanotube, but the dark region in the core of the nanotube still appeared in the TEM image in Figure 5d. If the core of the nanotube is completely hollow, the contrast inside the nanotube should appear as a lighter color, as shown in the TEM image of the neat template nanotube (Figure 1a). Therefore, when the lower concentration of Au ion was incubated onto the nanotubes, Au nanocrystals were grown only inside the nanotubes.

To confirm that the sequenced peptide is responsible for the regulations of the size and the packing density of Au nanocrystals, TEM images of Au coatings on the template nanotubes in the same experimental conditions without the sequenced histidine-rich peptide were compared to the ones with the histidine-rich peptide on the nanotubes. Figure 5e is a TEM image of Au nanocrystals grown without the histidine-rich peptide after incubating Au ions at pH 8 for 4 days. Au nanocrystals grown in this condition were polydisperse in the diameter range between 5 and 50 nm, while Au nanocrystals grown with the histidine-rich peptide were monodisperse in a diameter of 6 nm (Figure 5b). When Au ions were reduced without the histidine-rich peptide after incubating Au ions in the pH 8 solution for 12 days, Au nanocrystals were no longer observed, and the Au coating became continuous on the nanotube as shown in Figure 5f. In the same experimental condition with the histidine-rich peptide, Au nanocrystals were still monodisperse on the nanotubes, as shown in Figure 5a.

Discussion

When the template nanotubes were coated with Au without the sequenced histidine-rich peptide on the nanotube surfaces, Au nanocrystals were polydisperse (Figure 5e). After the longer

(60) Packing density of Au nanocrystals on nanotubes was calculated as (total area of Au nanocrystals)/(total area of nanotube surface) × 100. The areas were determined by TEM images of Au nanocrystals on the outer surfaces of nanotubes.

(61) Forster, S.; Antonietti, M. *Adv. Mater.* **1998**, *10*, 195.

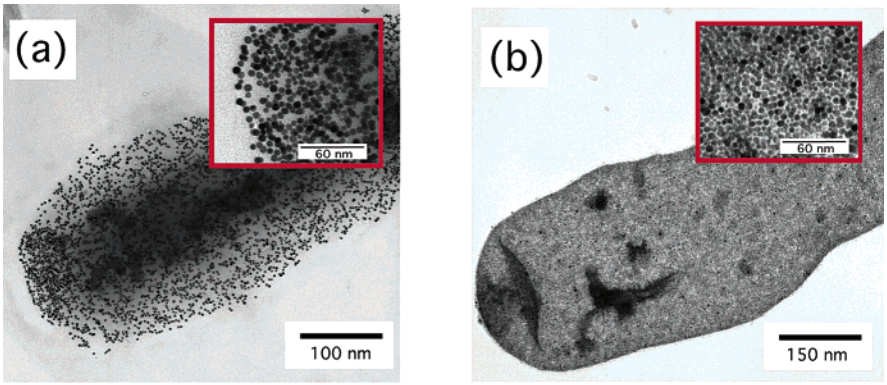

Figure 4. TEM images of Au nanocrystals on the sequenced histidine-rich peptide nanotubes grown by reducing the Au ion−nanotube solution after incubating Au ions for 10 days at (a) pH = 8 and (b) pH = 11.5. Insets show the TEM images in higher magnification.

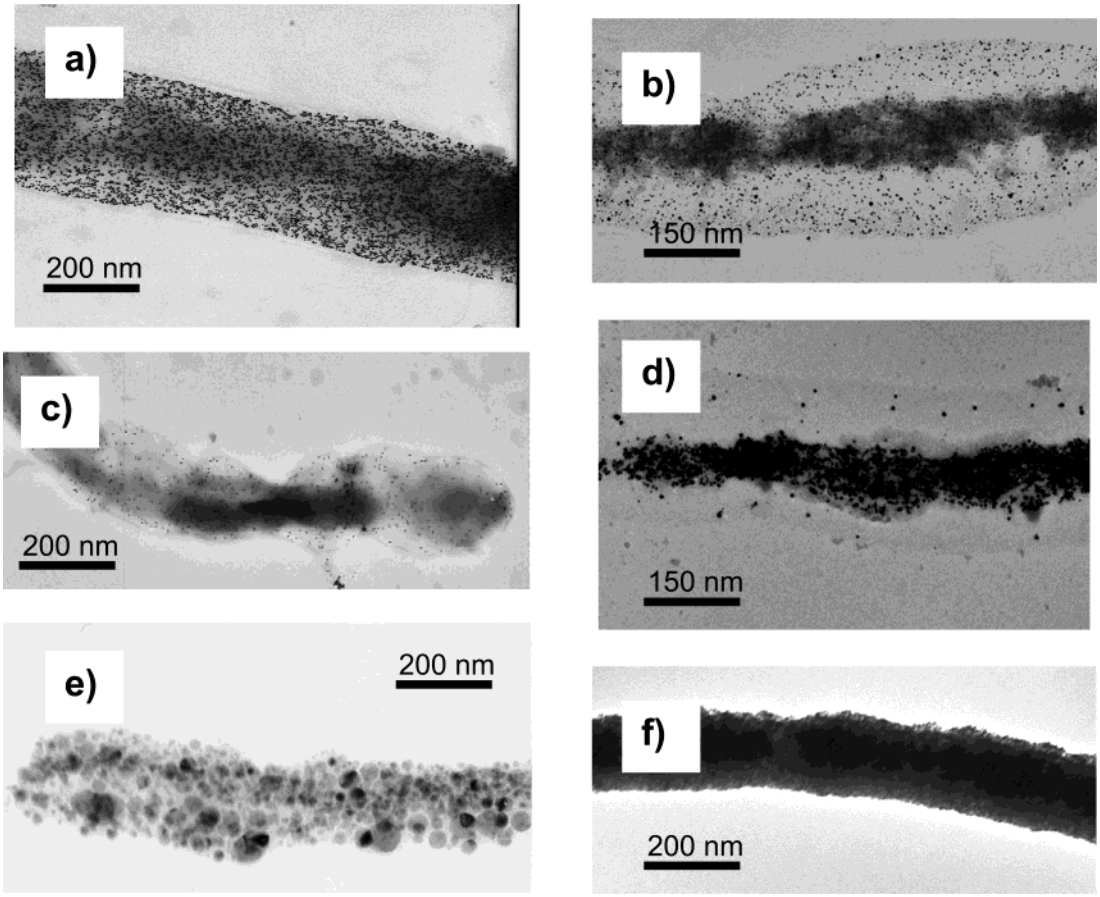

Figure 5. TEM images of Au nanocrystals on the sequenced histidine-rich peptide nanotubes grown by reducing the Au ion−nanotube solution (pH 8) after incubating Au ions for (a) 12 days, (b) 4 days, (c) 2 days, and (d) 5 h. TEM images of Au grown on the template nanotubes in the same experimental conditions without the sequenced histidine-rich peptide are also shown in (e) 4 day- and (f) 12 day-ion incubations.

ion incubation time period without the sequenced peptide, Au coated the entire nanotube surface continuously (Figure 5f). In the same experimental conditions with the histidine-rich peptide, monodisperse and discrete Au nanocrystals 6 nm in diameter were observed on the nanotube surfaces (Figure 5a and 5b). These comparisons indicate that the sequenced histidine-rich peptide regulates the size distribution of Au nanocrystals on the nanotubes.

As shown in Figures 4 and 5, both the pH change and the Au ion concentration change in the growth solutions have no effect on the size of Au nanocrystals grown on the histidine-rich peptide nanotubes. Under those condition changes, Au nanocrystals were always observed as being 6 nm in diameter. The size change and the morphology change of nanocrystals are expected to be observed when the mineralizing peptide molecules undergo conformation changes.[54] Since the pH change alters peptide−ion interactions, mainly due to the charge distribution changes in electron donor groups of peptides,[51] the altered interactions between peptides and ions induce the chemical structure change of the ion−peptide complexes, which determines the size and the morphology of nanocrystals after reducing those ions. Because the size change of Au nanocrystals on the nanotubes was not observed in Figure 4, it indicates that there is no major conformation change of the sequenced histidine-rich peptide molecules on the nanotubes in the pH range examined in this study. The rigidness of the peptide

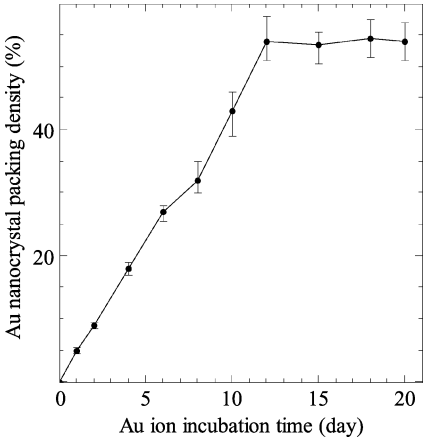

Figure 6. The correlation between the packing density of Au nanocrystals and the Au ion incubation time in the growth solution at pH = 8.

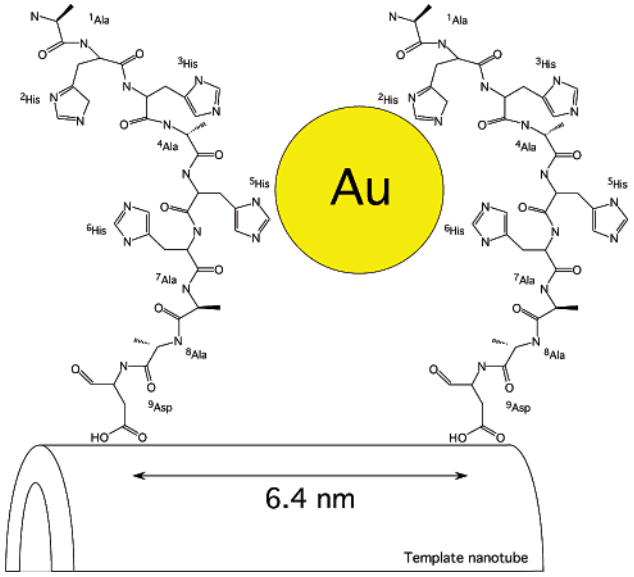

Figure 7. A proposed structure of the Au nanocrystal−peptide complex on the template nanotube.

backbones on the nanotubes was also supported by Raman spectroscopy. While the C−N stretch and the Au−N stretch modes (1261 and 1430 cm^{-1}) are sensitive to the peptide conformational changes via aggregations,[62,63] no frequency shifts of the peptide vibrations including those modes were observed among different pH solutions (Supporting Information). The size of Au nanocrystals, 6 nm in diameter, is consistent with the spacing of histidine-rich peptide molecules on the nanotubes. The periodicity of amide groups on the nanotubes to bind the histidine-rich peptides is 6.4 nm in distance,[56] and this peptide spacing seems to determine the size of Au nanocrystals.[54] As illustrated in Figure 7, the sequenced histidine-rich peptide molecules on the nanotubes likely trap Au nanocrystals and limit their growth to 6 nm in diameter. Generally, peptides with greater degrees of rotational freedom in the peptide backbone can trap and grow a variety of nanocrystal sizes.[64] The

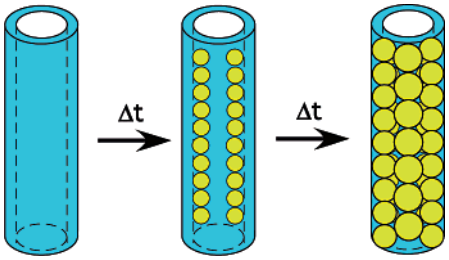

Figure 8. Sequence of the Au nanocrystal growth on the histidine-rich peptide nanotube surfaces.

sequenced peptide used in this report may be too rigid to produce various nanocrystal sizes on the nanotube surfaces.

The packing density change of Au nanocrystals via the pH change in the growth solution is explained by electron donor groups in the sequenced peptide.[51] In the lower pH range, the imidazole of the histidine residue binds Au ions strongly. In the higher pH range, the amine of the alanine residue can donate electrons and anchor Au ions, while the imidazole groups still bind Au ions. More binding sites are available to anchor Au ions in the higher pH range, and therefore the higher density of the nucleation sites for Au nanocrystals results in the less defects and the higher packing density of the Au nanocrystals on the nanotubes. Generally, the metal ions bind amine sites of histidine-rich peptides in the pH range between 7 and 10,[51] which is consistent with our observation that the significant change in the packing density of Au nanocrystals occurred at pH 9.

It is reasonable to observe the increase in the Au nanocrystal packing density with the higher Au ion concentrations on the nanotubes due to the larger number of nucleation seeds for Au nanocrystal growth. Therefore, the decrease of Au nanocrystal packing density was observed when the Au ion incubation time was reduced. Over 12 days, the increase in the packing density of Au nanocrystals was no longer observed, and it indicates that the binding sites on the histidine-rich peptide nanotubes are saturated after incubating Au ions for 12 days. It is interesting to observe that the Au nanocrystals were also grown inside the nanotubes and we could limit the Au nanocrystal growth only inside the nanotubes when the Au ion incubation time was reduced to 5 h. This observation suggests the coating mechanism that the Au nanocrystals grow inside the nanotubes first and then grow on the outer surfaces, as illustrated in Figure 8. We do not clearly understand this growth mechanism, while this outcome indicates that multiple materials can be coated inside and outside the nanotubes, respectively, which is very useful to design complex nanometer-scaled devices.

Conclusion

A sequenced histidine-rich peptide, A-H-H-A-H-H-A-A-D, was immobilized on the template nanotube surfaces, and this peptide regulated the size and the packing density of isotropic Au nanocrystals on the nanotubes. The conformations and the charge distributions of the histidine-rich peptide, controlled by the pH and the Au ion concentration in the growth solution, determine the size and the packing density of Au nanocrystals. The diameter of Au nanocrystals was 6 nm in various pH's and Au ion concentrations examined in this study. The spacing between the neighboring histidine-rich peptides on the nanotubes is 6.4 nm, and this geometry seems to limit the growth of Au

(62) Miura, T.; Hori-i, A.; Mototani, H.; Takeuchi, H. *Biochemistry* **1999**, *38*, 11560.
(63) Miura, T.; Suzuki, K.; Kohata, N.; Takeuchi, H. *Biochemistry* **2000**, *39*, 7024.
(64) Winges, D. R.; Cameron, C. T.; Mehra, R. K. *Metallothioneins: Synthesis, Structure, and Properties of Metal-Iothioneins, Phytochelatins, and Metal Complexes*; VCH: New York, 1992.

nanocrystals to 6 nm in diameter. As the growth solution was adjusted to higher pH's, the packing density of Au nanocrystals increased, while the nanocrystal size remained constant. The increase of Au nanocrystal packing density at higher pH's is consistent with the increase of Au ion binding sites in the sequenced histidine-rich peptide because amine groups of the alanine residue contribute as electron donors to Au ions at higher pH's in addition to the imidazole groups of the histidine residue. Therefore, more nucleation sites in the histidine-rich peptide at higher pH's induce the less defects in the Au nanocrystal assembly. The increase of the Au ion concentration also resulted in the higher packing density of Au nanocrystals on the nanotubes. TEM images of Au nanocrystals on the nanotubes grown in the shorter Au ion incubation time periods reveal that Au nanocrystals grow inside the nanotubes first and then cover the outer surfaces of the nanotubes. Therefore, multiple materials will be coated inside and outside the nanotubes, respectively, by controlling doping ion concentrations and their deposition sequences.

An advantage to applying biological recognitions to synthesize metal nanocrystals on nanotubes is the efficient and reproducible nanocrystal production in the control of size and packing density without contaminating with precipitated metal aggregates. This is important when those nanotubes are practically used as the building blocks for electronics and sensor devices because uniform metal coatings with the small and monodisperse domain sizes are crucial to optimize nanotube conductivity and to detect changes in conductivity and absorption induced by analyte adsorption on metal nanotube surfaces.[23,65] Metallic nanocrystals in diameter of 6 nm are in the size domain to observe a significant conductivity change by changing the packing density of nanocrystals. While the size of Au nanocrystals is constant in various experimental conditions examined in this study, different sequences of peptides with more flexible backbones will allow us to tune the size of nanocrystals in various pH's.

We believe this simple metal nanotube fabrication method via biomineralization can be applied to various metals and semiconductors with peptides whose sequences are known to mineralize specific ions. Peptide nanotubes incorporated with a recognition protein (antibody) have been used to assemble the nanowires onto patterned complementary protein (antigen) surfaces via biological recognition.[66] Therefore, a combination of sequenced peptides and proteins on nanotubes that control biological mineralizations and biological immobilizations may produce various structures of electronics and sensor devices in a simple and economical manner.

Acknowledgment. This work was supported by the National Science Foundation CAREER Award (ECS-0103430) and the U.S. Department of Energy (DE-FG-02-01ER45935). R.D. acknowledges Professor William L'Amoreaux (Department of Biology, CUNY College of Staten Island) for technical support of TEM.

Supporting Information Available: Raman spectra of the histidine-rich peptides on the nanotubes in various pH's of the Au ion solutions (PDF). This material is available free of charge via the Internet at http://pubs.acs.org.

JA0299598

(65) Sample, J. L.; Beverly, K. C.; Chaudhari, P. R.; Remacle, F.; Heath, J. R.; Levine, R. D. *Adv. Mater.* **2002**, *14*, 124.
(66) Matsui, H.; Porrata, P.; Douberly, G. E. J. *Nano Lett.* **2001**, *1*, 461.